Electronic Supplementary Material (ESI) for Organic & Biomolecular Chemistry.

Supporting Information

The Inverting Mechanism of the Metal Ion-Independent LanGT2: The First Step to Understand the Glycosylation of Natural Product Antibiotic Precursors through QM/MM Simulations

Fernanda Mendoza[*a] and Gonzalo A. Jaña [*a]

[a] Departamento de Ciencias Químicas, Facultad de Ciencias Exactas, Universidad Andres Bello, Autopista Concepción-Talcahuano 7100, Talcahuano, Chile.

[*]**E-mail:** m.mariafernandamendo@uandresbello.edu or
[*]**E-mail:** gonzalo.jana@unab.cl

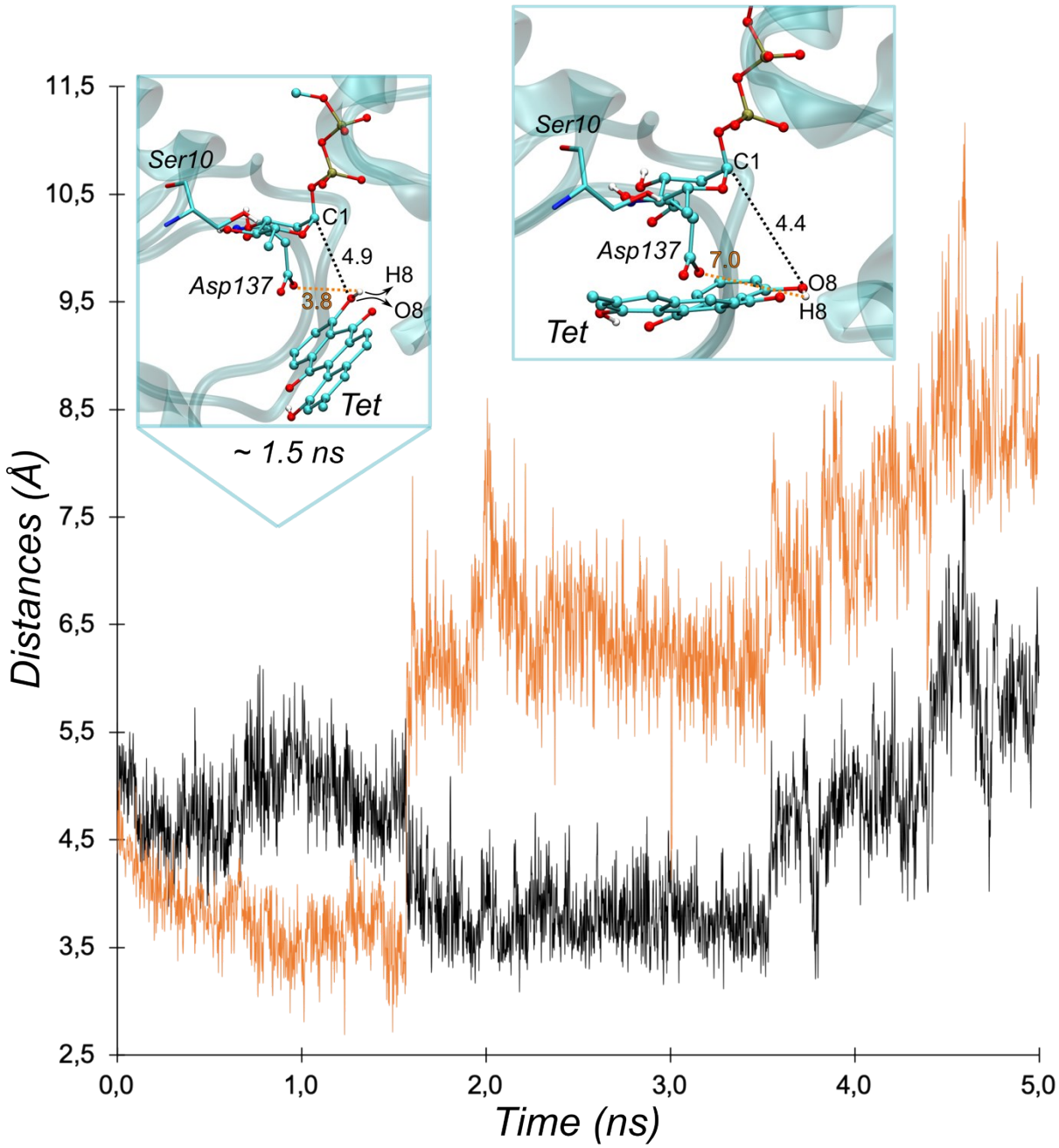

Fig. S1 Representation of the Michaelis complex modeled through MD simulations without restrains applied on the catalytic distances. The temporal variation of important distances, such as: the nucleophilic attack (C1-O8) and putative nucleophilic activation (H8-Asp137) are depicted in black and orange colors, respectively. The molecular representations of the Michaelis complex show the average value of the C1-O8 (black) and the H8-Asp137 (orange) distances during the first 1.5 ns (top left panel), and during last 3.5 ns (top right panel) of simulation.

As shown in Figure S1, if there is no restraint on the $C1_{Oli}$-$O8_{Tet}$ distance the hydroxyl nucleophilic moiety of tetrangulol (Tet) orients to the closer oxygen in the structure of Tet (intramolecular interaction). Besides, during the last nanoseconds the hydroxyl nucleophilic moiety moves further away from the base catalyst Asp137, exhibiting a distance of approximately 7 Å which is not a catalytic configuration.

Table S1. Potential energy profiles for models 1 and 2 using different QM fragments, calculated at the QM(BP86/6-31G+(d))/CHARMM(MM) level. All values are given in kcal mol^{-1}.

	Model 1		**Model 2**
	QM1 fragment	**QM2 fragment**	**QM1 fragment**
$\Delta E^{\ddagger}$	34	29	54
HES distances (Å)	**Model 1**		**Model 2**
	QM1 fragment	**QM2 fragment**	**QM1 fragment**
$C1_{Oli}$ - O_G	2.56	3.17	2.28
$C1_{Oli}$ - $O8_{Tet}$	2.01	2.00	2.36
$C1_{Oli}$ - $O5_{Oli}$	1.33	1.31	1.31
$C8_{Tet}$ - $O8_{Tet}$	1.33	1.36	1.30
$H8_{Tet}$ - O_W	1.05	1.26	0.99
H_W - $O1_{Asp137}$	1.05	1.41	1.01
H_S - O_G	1.77	1.53	9.81
$H3_{Oli}$ – $O2\alpha$	1.76	1.67	8.68

Table S2. Potential energy barriers and energy reactions at different levels of theory for the O-glycosylation mechanism. All values are given in kcal mol^{-1}. The reactant, TS and product structures were optimized at the QM(BP86/6-31G(d))/CHARMM(MM) level.

QM Method	$\Delta E^{\ddagger}$	ΔE
BP86/6-31G(d)	18.1	9.3
BP86/6-311G(d,p)	17.5	8.9
M06-2X/6-31G(d)	25.8	9.5
M06-2X/6-311G(d,p)	24.9	9.4
M06-2X/6-311G++(d,p)	27.1	8.4
ωB87X-V/6-31G(d)	26.2	10.0
ωB87X-V/6-311G(d,p)	25.2	9.6
ωB87X-V/6-311G++(d,p)	27.7	8.2

Table S3. Distances (in Å) calculated for the States Located along the MEP at the QM(BP86/6-31G(d))/MM(CHARMM) level (see Figure S1).

Distances (Å)	**R**	**TS**	**P**
H_S[Ser219] – O1α	1.97	1.93	1.90
H_N[Ser219] – O1α	1.71	1.68	1.68
N1[Arg220] – O1α	2.86	2.79	2.82
N2[Arg220] – O1β	2.65	2.63	2.64
N_2[His283] – O2α	2.71	2.65	2.65

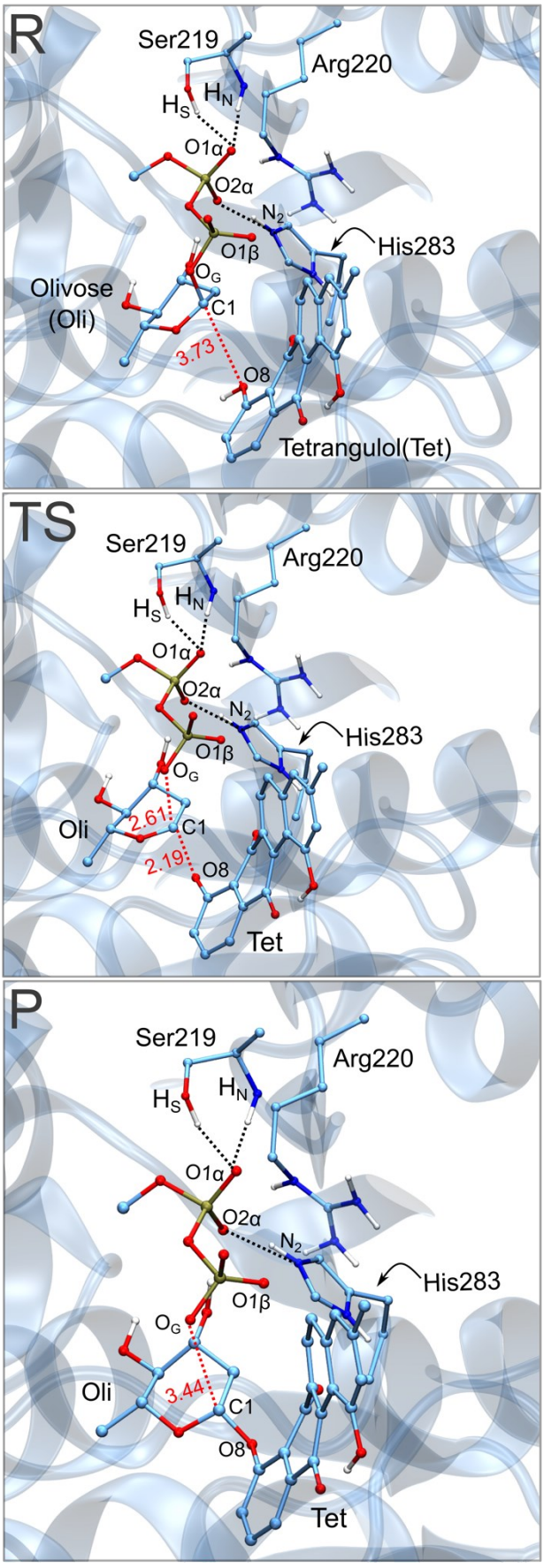

Fig. S2 QM/MM modeling of the MEP for the inverting glycosylation mechanism catalyzed by O-LanGT2: Reactant (R), transition state (TS) and product (P) structures. In order to highlight the protein-diphosphate interactions, W_{cat} is not shown in any of the panels. The interactions between the diphosphate with the Ser219 and His283 are depicted as dotted black lines. Breaking-forming bonds are represented by dotted red lines.[a]

[a] See the values of the distances in Table S3